

# Investigation of Particle–Molecule Interactions by Use of a Dielectric Continuum Model

Marianne Sloth,<sup>\*,†</sup> Solvejg Jørgensen,<sup>‡,§</sup> Merete Bilde,<sup>†,||</sup> and Kurt V. Mikkelsen<sup>†,⊥</sup>

Department of Chemistry, H. C. Ørsted Institute, University of Copenhagen, DK-2100 Copenhagen Ø, Denmark, and The Fritz Haber Research Center of Molecular Dynamics, Hebrew University, Jerusalem 91904, Israel

Received: April 30, 2003; In Final Form: July 8, 2003

We develop a model that describes a molecule interacting with an aerosol particle using a modified heterogeneous solvation model. The particle is represented as a dielectric medium characterized by a macroscopic dielectric constant. The dielectric constant depends on average composition and temperature. We utilize the model to investigate the interactions between an aqueous particle and a succinic acid molecule. We show how interaction energies and linear response properties depend on the orientation of the organic dicarboxylic acid relative to the particle surface and on the dielectric properties of the particle. The long-term goal of our work is the calculation of sticking coefficients.

## I. Introduction

To model mass and heat transfer to and from atmospheric particles, it is essential to know what happens to a gas molecule when it encounters the surface of a particle.<sup>1</sup> On a macroscopic level the so-called sticking probabilities/mass accommodation coefficients are used to model evaporation, condensation, and heterogeneous chemistry in the atmosphere.

The sticking probability has proven to be an important parameter for prediction of climate parameters such as the concentration of cloud condensation nuclei. For example, Pandis, Russel, and Seinfeld<sup>2</sup> showed that changing the accommodation coefficient for sulfuric acid from 0.02 to 0.05 in their nucleation and growth model for aerosols in the marine boundary layer reduced the calculated concentration of cloud condensation nuclei by 45%.

Clement et al.<sup>3</sup> have analyzed experimental data and proposed a simple model that describes the interaction as a two-body collision in which energy and momentum are exchanged. This model generally predicts sticking probabilities close to one. In accordance with this, Kulmala and Wagner<sup>4</sup> have suggested using sticking probabilities of one if no other experimentally verified information is available.

The problems associated with the understanding and estimation of the probability of adsorption and condensation of a molecule approaching an aerosol particle have been clearly demonstrated in refs 2, 3, and 5–10. The theoretical approaches range from total phenomenological approaches to microscopic molecular models.<sup>2,3,5–10</sup> The phenomenological approaches utilize thermodynamic arguments for evaluating the energy terms that enter the macroscopic expression for the transition state theory rate constant of the sticking process.<sup>9,10</sup> Another view within the phenomenological methods is the one based on pure statistical models for the nucleation of aerosols. Generally, it is

clear that these models do not utilize or provide a molecular understanding of the considered processes. A fair number of models exist for describing the interactions of a spherical and classical particle scattering off a plane, isotropic, homogeneous surface. These models do not include any molecular detail and will never be able to differentiate among different molecules, except on the basis of size and mass.<sup>3</sup> On the other hand, the microscopic models cover methods where a small number of molecules interact with the approaching molecule. These models enable a molecular understanding of the changes in the structures and properties of the approaching molecule. Unfortunately, the very small number of molecules included in the models renders these approaches insufficient with respect to an appropriate description of the bulk properties of the aerosol particle.<sup>6–8</sup> The number of models that utilize a bulk description of the aerosol particle and a quantum mechanical method for the approaching molecule is limited. We are only aware of the method presented in this article and the one we presented in ref 53.

The above considerations suggest that there is a need for microscopic models to provide an understanding of the interactions between gas molecules and atmospheric particles on the molecular level. The long-term goal of our work is to provide such an understanding. Our first step has been to use *ab initio* calculations to study how an organic molecule interacts with an atmospheric particle represented as a homogeneous dielectric medium. For this purpose we have modified a heterogeneous solvation model originally developed to calculate interaction energies and time-dependent properties of a solvated molecule in a dielectric film absorbed on a metallic surface.<sup>11–13</sup>

It is a method that enables the modeling of molecules at macroscopic surfaces, and as shown in ref 14, it is a reliable model for investigating surface science issues related to molecules on metal surfaces.

The organic molecule studied in this work is succinic acid (1,4-butanedioic acid), which has been observed as one of the most abundant dicarboxylic acids in photochemical smog.<sup>15–17</sup> The average particle chemical composition is represented by a macroscopic dielectric constant. Interaction energies and linear response properties are important indicators for particle–molecule interactions, and we show how they

\* To whom correspondence should be addressed. Electronic mail: ms@theory.ki.ku.dk.

† University of Copenhagen.

‡ Hebrew University.

§ Electronic mail: solvejg@fh.huji.ac.il.

|| Electronic mail: mbilde@kiku.dk.

⊥ Electronic mail: kmi@theory.ki.ku.dk.

depend on the orientation of the organic dicarboxylic acid relative to the particle surface and on the dielectric constant of the particle.

In the following, we first (section II) describe the theoretical background for the dielectric continuum model and then present interaction energies and molecular properties in section III. Finally, the performance and limitations of the aerosol model are discussed in section IV.

## II. Theory

A number of models have been developed that describe a molecule subjected to an outer environment. The main principle of these models is to divide the system into at least two subsystems that are treated at different levels of theory. Whereas quantum mechanical/molecular mechanical (QM/MM) models keep the reference to the discrete molecules,<sup>18–22</sup> the main part of the existing models represents the outer environment as a dielectric medium.<sup>11–13,23–31</sup> The heterogeneous solvation model developed in refs 11–13 operates with three subsystems: A molecule is enclosed in a half-spherical cavity and the flat surface of the cavity is absorbed on a metal surface while the spherical surface is exposed to a solvent. The metal is represented as a perfect conductor, and the solvent, by a dielectric medium which is homogeneous, isotropic, polarizable, and characterized by the scalar, static dielectric constant  $\epsilon$ . This model has been used to investigate how heterogeneous solvation influences the molecular properties of carbon monoxide and benzene.<sup>11–13</sup>

To study the interactions between an atmospheric particle and a gas-phase molecule, we have modified the heterogeneous solvation model as follows: we neglect the dielectric film (solvent) and replace the perfect conductor by a dielectric surface which represents the particle. The modified model enables us to describe a molecule which interacts with an atmospheric particle, represented by a dielectric surface.

**A. Model.** The aerosol is represented by a semi-infinite dielectric medium, and the coordinate system is defined so that the medium is confined to  $z < 0$  while the molecular system is located outside the aerosol ( $z > 0$ ). From the solution of the wave function for the molecular system we represent the molecule by its discrete molecular charge distribution where a partial charge is assigned to each atom of the molecule. The molecular partial charges are determined as proposed in the work by Cioslowski.<sup>32,33</sup> We assume that the vacuum–dielectric medium interface is located at  $z = 0$  and consider a point charge  $q_i$  placed at  $\vec{r}_i = (x_i, y_i, z_i)$ , where  $z > 0$ .

The effect of the dielectric medium is then simulated by an image charge

$$q_{i,s} = -\frac{\epsilon - 1}{\epsilon + 1}q_i \quad (1)$$

$$\text{at } \vec{r}_{i,s} = (x_i, y_i, -z_i)$$

in the dielectric medium. The subscript *s* refers to an image charge. The positions of a partial charge  $q_i$  and its corresponding image charge  $q_{i,s}$  are sketched in Figure 1.

The induced potential from *N* partial charges at an arbitrary point,  $\vec{r}$ , in the vacuum region is given by

$$U_{\text{pol}}(\vec{r}) = \sum_{i=1}^N U_{\text{pol}}^{(i)}(\vec{r}) = \sum_{i=1}^N \frac{q_{i,s}}{|\vec{r} - \vec{r}_{i,s}|} \quad (2)$$

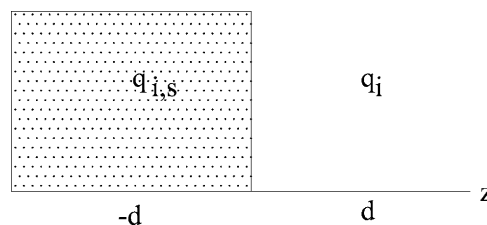


**Figure 1.** Position of a partial charge  $q_i$  and its corresponding image charge  $q_{i,s}$ .

The resulting energy due to the interaction between the discrete molecular charge distribution,  $\rho_m(\vec{r})$ , and the dielectric medium is

$$E_{\text{pol}} = \frac{1}{2} \int d\vec{r} \rho_m(\vec{r}) U_{\text{pol}}(\vec{r}) \quad (3)$$

Using this expression, the polarization interaction operator becomes

$$\hat{W}_{\text{pol}} = \sum_j \sum_k U_{\text{pol}}^{(k)}(\vec{r}_j) \sum_{pq} \langle \phi_p | q_j | \phi_q \rangle E_{pq} \quad (4)$$

where  $|\phi_p\rangle$  and  $|\phi_q\rangle$  represent molecular orbitals and the orbital excitation operator,  $E_{pq}$ , is defined as

$$E_{pq} = \sum_{\sigma} a_{p\sigma}^{\dagger} a_{q\sigma} \quad (5)$$

The operators  $a_{p\sigma}^{\dagger}$  and  $a_{q\sigma}$  are the electron creation and annihilation operators, respectively, and the set  $\{|\phi_p\rangle\}$  represents a set of orthonormal orbitals.

The wave function and energy of the molecular system in the presence of the aerosol are determined by solving the electronic Schrödinger equation for a fixed nuclear configuration

$$(\hat{H}_M^{\circ} + \hat{W}_{\text{pol}})|0\rangle = E|0\rangle \quad (6)$$

with  $\hat{H}_M^{\circ}$  being the Hamiltonian for the molecular system in a vacuum.

The Schrödinger equation is solved self-consistently using ab initio methods.

**B. Response Theory.** Response theory as developed and presented in refs 34–37 has clearly shown the possibilities of calculating time-dependent electromagnetic properties at different levels of electronic structure theory. The focus of response theory has mainly been computing static and dynamic molecular properties of molecules in the gas phase.<sup>38–45</sup>

The heterogeneous solvation model enables the calculation of time-dependent molecular response properties and thus facilitates an investigation of the influence of an aerosol particle on the properties of a molecular system. Here, we consider the response of the molecular system to a time-dependent perturbation.

The response of the molecular system to a time-dependent perturbation,  $V(t)$ , is determined by requiring the Ehrenfest equation to be fulfilled in all powers of the perturbation<sup>46</sup>

$$\frac{d\langle \tilde{0} | \hat{A} | \tilde{0} \rangle}{dt} = \left\langle \tilde{0} \left| \frac{\partial \hat{A}}{\partial t} \right| \tilde{0} \right\rangle - i \langle \tilde{0} | [\hat{A}, \hat{H}(t)] | \tilde{0} \rangle \quad (7)$$

The time-dependent Hamiltonian is given by

$$\hat{H}(t) = \hat{H}_M^{\circ} + \hat{W}_{\text{pol}} + V(t) \quad (8)$$

and a general perturbation operator,  $V(t)$ , in the frequency domain is expressed by

$$V(t) = \int_{-\infty}^{\infty} d\omega V^\omega \exp[(-i\omega + \epsilon)t] \quad (9)$$

where  $\epsilon$  is a positive infinitesimal number ensuring that the perturbation is switched on adiabatically at  $t = -\infty$ . The frequency is denoted  $\omega$ , and  $V^\omega$  is the Fourier transform of  $V(t)$ . It is assumed that the time-dependent wave function  $|\tilde{0}\rangle$  is an eigenfunction  $|0\rangle$  of  $(\hat{H}_M^\circ + \hat{W}_{\text{pol}})$  at  $t = -\infty$ .

The time-development of an expectation value of a time-independent operator  $\hat{A}$  may be expanded as<sup>46</sup>

$$\langle \tilde{0} | \hat{A} | \tilde{0} \rangle = \langle 0 | \hat{A} | 0 \rangle + \int_{-\infty}^{\infty} d\omega \exp[(-i\omega + \epsilon)t] \langle \langle A; V^\omega \rangle \rangle_\omega + \frac{1}{2} \int_{-\infty}^{\infty} d\omega_1 \int_{-\infty}^{\infty} d\omega_2 \exp[(-i(\omega_1 + \omega_2) + 2\epsilon)t] \langle \langle A; V^{\omega_1}, V^{\omega_2} \rangle \rangle_{\omega_1, \omega_2} + \dots \quad (10)$$

where the linear response function  $\langle \langle A; V \rangle \rangle_\omega$  contains all contributions that are linear in the perturbation and the quadratic response function  $\langle \langle A; V^{\omega_1}, V^{\omega_2} \rangle \rangle_{\omega_1, \omega_2}$  contains all terms quadratic in the perturbation.

The expectation values are determined from the time-dependent Hartree–Fock wave function  $|\tilde{0}\rangle$ <sup>46</sup>

$$|\tilde{0}\rangle = \exp(i\kappa(t)) |0_{\text{HF}}\rangle \quad (11)$$

where  $|0_{\text{HF}}\rangle$  fulfills the generalized Brillouin condition and  $\exp(i\kappa(t))$  describes a unitary transformation in orbital space

$$\kappa(t) = \sum_k [\kappa_k(t) c_k^\dagger + \kappa_k'(t) c_k] \quad (12)$$

The orbital excitation operators  $c_k^\dagger$  are defined as

$$c_k^\dagger = E_{pq} = a_{p\alpha}^\dagger a_{q\alpha} + a_{p\beta}^\dagger a_{q\beta}, \quad p > q \quad (13)$$

The operators to be considered in the Ehrenfest equation are the set of operators describing the time evolution

$$\tilde{T} = (\tilde{c}^\dagger, \tilde{c}) \quad (14)$$

where the time-transformed operators are given by

$$\tilde{c}_k^\dagger = \exp[i\kappa(t)] c_k^\dagger \exp[-i\kappa(t)] \quad (15)$$

One term arises due to the interaction with the dielectric medium and describes the changes of the response functions due to the presence of the induced charges in the dielectric medium. Inserting the expression for the polarization operator, the polarization contribution to the Ehrenfest equation may be written as

$$-i \langle \tilde{0} | [\tilde{T}^\dagger, \hat{W}_{\text{pol}}] | \tilde{0} \rangle = -i \sum_j \sum_k U_{\text{pol}}^{(k)}(\vec{r}_j) \sum_{pq} \langle \phi_p | q_j | \phi_q \rangle \langle \tilde{0} | [\tilde{T}^\dagger, E_{pq}] | \tilde{0} \rangle \quad (16)$$

Linear and higher order contributions may be found by expanding  $|\tilde{0}\rangle$  and  $\tilde{T}^\dagger$ .

$$-i \langle \tilde{0} | [\tilde{T}^\dagger, \hat{W}_{\text{pol}}] | \tilde{0} \rangle = G^{(0)}(\tilde{T}^\dagger) + G^{(1)}(\tilde{T}^\dagger) + G^{(2)}(\tilde{T}^\dagger) + G^{(3)}(\tilde{T}^\dagger) + \dots \quad (17)$$

Only terms linear in  $\kappa(t)$  enter in the case of the Hartree–Fock linear response.

Considering the operator,  $\tilde{c}_k^\dagger$ , we obtain

$$G^{(1)}(\tilde{c}_k^\dagger) = - \sum_j \sum_k U_{\text{pol}}^{(k)}(\vec{r}_j) \sum_{pq} \langle \phi_p | q_j | \phi_q \rangle \langle 0 | [c_k^\dagger, [\kappa(t), E_{pq}]] | 0 \rangle \quad (18)$$

The contribution is similar to that obtained for the operator  $\tilde{c}_k$  except that  $c_k^\dagger$  is replaced by  $c_k$ .

**C. Molecular Properties.** The response functions contain information about molecular properties. Evaluating expressions for the response functions in the case of an exact reference state enables a physical interpretation of the response functions. For an exact reference state  $|0\rangle$  and in a basis of eigenfunctions  $|n\rangle$  of  $H_0$ , the linear response function may be expressed as<sup>46</sup>

$$\langle \langle A; V^\omega \rangle \rangle_\omega = \lim_{\epsilon \rightarrow 0} \sum_{n \neq 0} \frac{\langle 0 | \hat{A} | n \rangle \langle n | V^\omega | 0 \rangle}{\omega - \omega_n + i\epsilon} - \lim_{\epsilon \rightarrow 0} \sum_{n \neq 0} \frac{\langle 0 | V^\omega | n \rangle \langle n | \hat{A} | 0 \rangle}{\omega + \omega_n + i\epsilon} \quad (19)$$

Replacing  $\hat{A}$  in eq 19 with the electric dipole operator gives an expression for the polarizability. Knowledge of the polarizability is important for the description of intermolecular forces, since both the induction and dispersion contributions to the energy depend on the polarizability. Furthermore, the polarizability is related to molecular reactivity. We note that a qualitative minimum polarizability principle has been formulated stating that the natural direction of evolution of any system is toward a state of minimum polarizability.<sup>47</sup>

### III. Results and Discussion

We consider a molecule of succinic acid (1,4-butanedioic acid) approaching an atmospheric particle. We calculate the interaction energies and linear response properties for different relative orientations. While the interaction energies are important for the calculation of sticking coefficients, the static polarizability influences the reactivity of the molecular system.

The gas-phase geometry of succinic acid was optimized at the MP2/6-311G\*\* level of theory. The optimization was performed without symmetry constraints. The optimized structure of succinic acid is almost symmetric, and all carbon and oxygen atoms are lying in the  $xy$ -plane. In the following we refer to this structure as the standard conformation. The carboxylic acid group pointing toward the dielectric medium is denoted A, and the carboxylic acid group pointing away is denoted B.

Figure 2 shows the four investigated orientations of the molecular system relative to the particle surface. The x and y orientations refer to the standard conformation approaching the dielectric medium side-on and end-on, respectively. For the end-on (y) orientation an extra series of calculations was performed with the molecule aligned so that the two oxygen atoms in carboxylic acid group A were parallel to the surface. This orientation is denoted y2. Finally, we performed a calculation series for another conformation of succinic acid where the two carboxylic acid groups are pointing toward the same direction (see Figure 2d). This molecular structure has a higher vacuum equilibrium energy than the standard conformation. The geometry of the rotated conformation is not obvious from Figure 2, since it is not a planar molecule, but the difference between the orientations should be clear.

We refer to the distance between succinic acid and the particle as the distance from the molecular center of mass to the surface

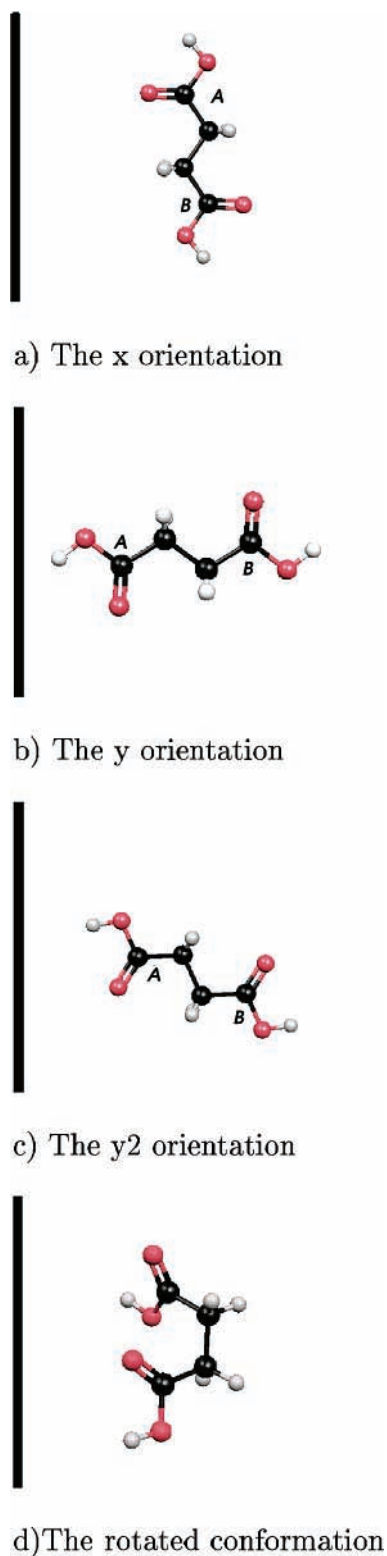


**Figure 2.** Orientation of succinic acid relative to the surface of the particle.

of the dielectric medium. Since we refer to the center of mass of the molecular system, it is possible to perform the calculations for the rotated conformation at shorter distances than those for the calculations for the standard orientations.

The optimization of the wave function and the calculation of linear response properties were performed with a local version of the program Dalton.<sup>48</sup> The calculations were performed in the  $C_1$  symmetry group at the HF/cc-pVDZ level of theory for different molecular orientations relative to the particle. The

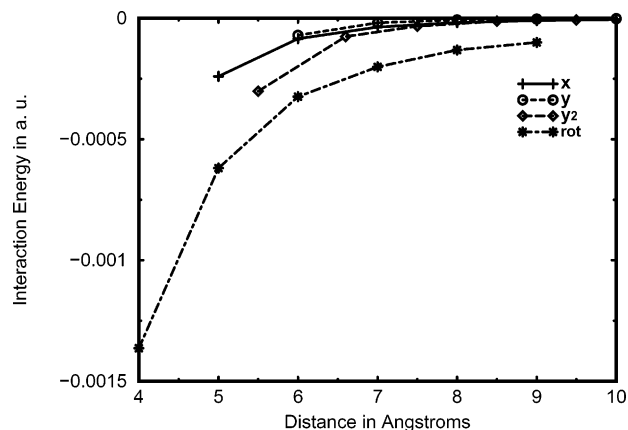


**Figure 3.** Interaction energies in au as a function of distance. The vacuum energy is  $-454.5061$  au for the standard and  $-454.5033$  au for the rotated conformation.  $1 \text{ au} = 2625.50 \text{ kJ/mol}$ .

image charges, given by eq 1, were calculated for  $\epsilon = 78.54$ , which is the static dielectric constant for water at  $25 \text{ }^\circ\text{C}$ .<sup>26</sup>

Interaction energies for different particle–molecule distances and orientations are calculated, and these are compared with the shift of the dipole moment, static polarizability, excitation energies, and dipole transition moments relative to the vacuum state. We define the shift of property  $A$  as

$$\Delta A = A - A_{\text{vac}} \quad (20)$$

where  $A$  is calculated in the presence of the dielectric medium and  $A_{\text{vac}}$  is the vacuum value. The dependence on the dielectric constant is studied for one orientation and different distances. Atomic units are used unless otherwise stated. Conclusions are based on trends in series of calculated numbers rather than absolute values.

**A. Interaction Energies.** The interaction energies obtained for the different orientations are presented in Figure 3. In all cases there is a weak attractive interaction that is largest for small distances. The interactions are similar to the ones encountered for very weak hydrogen bonding involved in intermolecular interactions in the gas phase. As expected, the energy is lowered most for the rotated conformation, but its total energy ( $E_{\text{total}} = E_{\text{vacuum}} + E_{\text{interaction}}$ ) is still higher than the total energies for the standard conformations.

To interpret the interaction energies, we consider the shift of the partial charges for the different orientations relative to the vacuum state as a function of distance from the particle surface. Figure 4 illustrates the shifts of the partial charges in group A and B for the x orientation. We note that carboxylic acid group A pointing toward the particle is affected differently from carboxylic acid group B, which points away from the particle.

To investigate this further, the individual contributions to the interaction energy from different parts of the molecule were calculated separately. The four partial charges in group A give rise to an attraction whereas group B contributes with a small repulsive interaction. The interaction with the alkane part of the molecule is also repulsive. The resulting interaction energy is attractive and becomes smaller as all terms fall off when the distance is enhanced. The large interaction energy calculated for the rotated conformation is due to an attractive contribution from both acidic groups.

A comparison between the obtained interaction energies for the y and y2 orientations (Figure 3) shows that the interaction with the medium is favored in the case of the y2 orientation. For both orientations the shifts of the partial charges as a function of distance vary nonuniformly, which implies that the



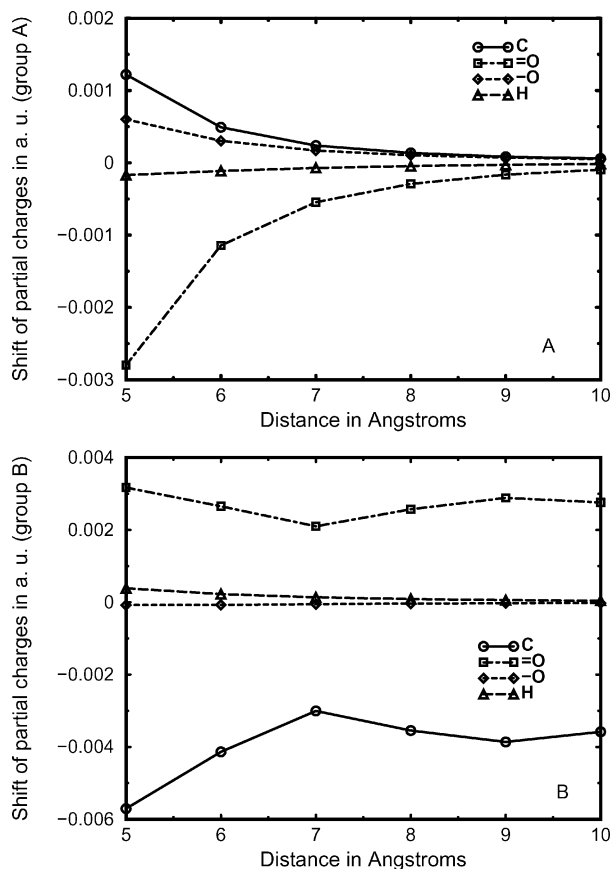


**Figure 4.** Shift of the partial charges in groups A and B as a function of the distance to the aerosol surface (*x* orientation). In a vacuum the partial charges are (au) (A)  $q_C = 1.2946$ ,  $q_{=O} = -0.8621$ ,  $q_O = -0.8180$ ,  $q_H = 0.3274$  and (B)  $q_C = 1.2945$ ,  $q_{=O} = -0.8620$ ,  $q_O = -0.8180$ ,  $q_H = 0.3273$ .

molecular charge distribution changes as a function of distance. This also reflects a significant anisotropic component of the interaction potential. Furthermore, the interaction energies are smaller than the corresponding solvation energies for similar systems;<sup>11–13,30,49,50</sup> the system is only solvated from one side.

In conclusion, the interaction energy is negative for all orientations but its magnitude depends on the relative orientation of the molecular system. Carboxylic acid groups pointing toward the dielectric medium enhance the interaction energy while carboxylic acid groups pointing away reduce the energy of interaction.

**B. Polarizability.** Figure 5 presents the shift of the mean polarizability for the three orientations of the standard conformation. The mean polarizability  $\bar{\alpha}$  is defined as

$$\bar{\alpha} = \frac{1}{3}(\alpha_{xx} + \alpha_{yy} + \alpha_{zz}) \quad (21)$$

In all cases the mean polarizability decreases as the diacid approaches the aerosol, that is, the diacid becomes harder to polarize. This is consistent with the principle of minimum polarizability.<sup>47</sup> A decrease of the mean polarizability is also observed for the rotated conformation.

The polarizability is related to the excitation energies and dipole transition moments, and these are therefore considered in the next section.

### C. Excitation Energies and Dipole Transition Moments.

Table 1 shows the excitation energies and corresponding dipole transition moments for the transitions from the ground state to the four lowest excited states as a function of the distance to

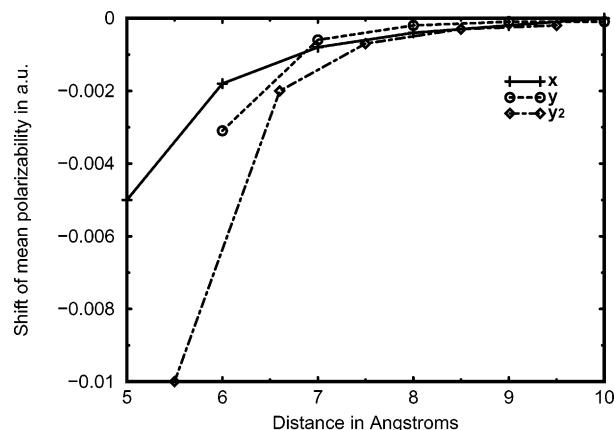


**Figure 5.** Shift of the mean polarizability as a function of distance. In a vacuum  $\bar{\alpha} = 47.6353$  au. The conversion factor is  $\alpha$  (cm<sup>3</sup>) =  $(0.148184 \times 10^{-24})\alpha(a_0^3)$ .

**TABLE 1: Excitation Energies and Dipole Transition Moments (TM) for the *x* Orientation in Atomic Units**

distance,	$E_{ex,1}$	$E_{ex,2}$	$E_{ex,3}$	$E_{ex,4}$	TM1	TM2	TM3	TM4
vacuum	0.2457	0.2462	0.3587	0.3874	0.107	0.000	1.089	0.001
10	0.2457	0.2462	0.3587	0.3580	0.107	0.003	1.088	0.013
9	0.2457	0.2462	0.3587	0.3580	0.107	0.004	1.088	0.020
8	0.2457	0.2462	0.3587	0.3580	0.107	0.006	1.088	0.031
7	0.2457	0.2463	0.3587	0.3580	0.107	0.010	1.088	0.054
6	0.2458	0.2463	0.3587	0.3580	0.106	0.019	1.084	0.103
5	0.2458	0.2465	0.3588	0.3580	0.101	0.036	1.067	0.214

the dielectric medium. The table also shows excitation energies in the absence of a dielectric (vacuum). The shifts of the excitation energies are different for the different transitions. Whereas the three lowest excited states are blue shifted (i.e. positive) when the molecule is close to the surface, the fourth is red shifted (i.e. negative) and the dielectric medium causes an interchange of the third and fourth excited states. This behavior reflects the fact that the presence of the dielectric medium affects the different excited states differently because their charge distributions and molecular properties differ from one another.

The dipole transition moments for the transitions to the first and third excited states are only slightly reduced in the presence of the dielectric medium and not until the molecule gets close to the surface. The second and fourth dipole transition moments are very small for the vacuum case but sensitive to the presence of the dielectric medium. They are slightly enhanced even at a distance of 10 Å and considerably enhanced at small distances. The effect is largest for the fourth excited state, where we also observed the largest shift of the excitation energy.

The same behavior is observed for the *y* and *y*<sub>2</sub> orientations, the only difference being the magnitude of the shift. For the rotated conformation we observe an increase of the four lowest excitation energies.

These results clearly illustrate that the interactions between the aerosol particle and the diacid are small compared to a similar situation where a molecule is solvated.<sup>11–13,30,49,50</sup>

The nonequilibrium situation that arises upon excitation of an electron may explain the general increase of the excitation energies. The excited state is not in equilibrium with the induced charges and is thus stabilized less by the dielectric medium, resulting in a larger excitation energy.

The increase of the excitation energies may partly explain the observed decrease of the mean polarizability because the excitation energies occur in the denominator of the sum-over-

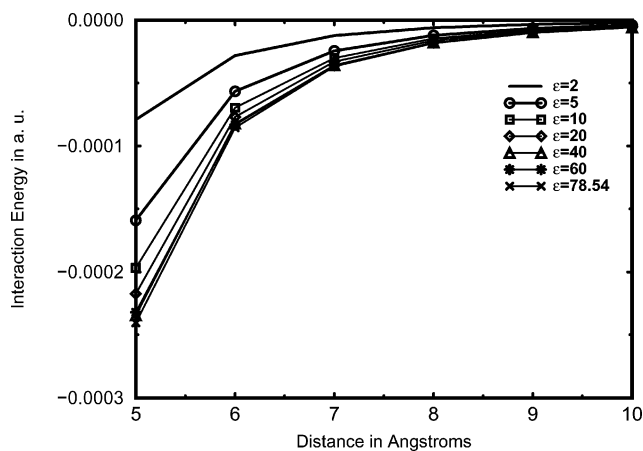


**Figure 6.** Dependence of the interaction energy on the dielectric constant as a function of distance.

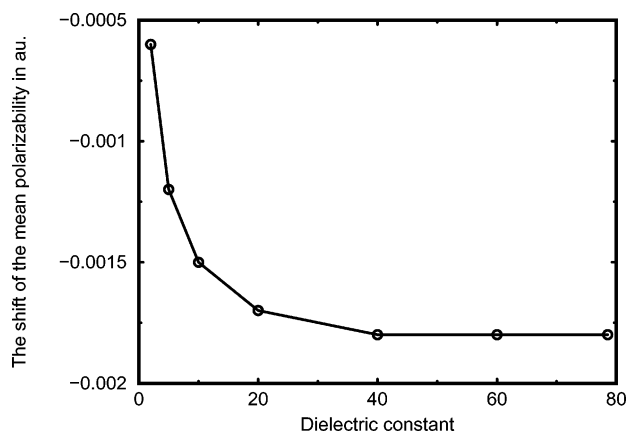


**Figure 7.** Dependence of the shift of the mean polarizability (au) on the dielectric constant at 6 Å.

states expression for the polarizability, which is a linear response property (eq 19).

**D. Dielectric Constant.** In this section we consider how the interaction energy and the molecular properties are affected when the dielectric constant is changed. For the *x* (side-on) orientation, calculations were performed for the following values of the dielectric constant,  $\epsilon = 2, 5, 10, 20, 40$ , and 60. For comparison the dielectric constant for ethanol is 24.30 (25°) and the dielectric constant for acetic acid is 6.15 at 20°. The obtained interaction energies are presented in Figure 6 along with those calculated for pure water,  $\epsilon = 78.54$ .

As expected from eq 1 the interaction energy increases when the dielectric constant is enhanced. The difference is largest for small particle–molecule distances and converges to zero for large distances. Furthermore, the effect of changing the dielectric constant is much more pronounced for small dielectric constants. This behavior may also be explained by inspection of eq 1, which shows that the charges are insensitive to small changes in the dielectric constant when it has exceeded a value of around 40. Similar behavior is observed when considering the shift of the mean polarizability (Figure 7).

#### IV. Conclusion

Assuming that a particle can be modeled as a homogeneous dielectric medium, the dielectric continuum model enables the calculation of interaction energies between an aerosol particle and an approaching molecule. Furthermore, it provides insight into the changes of the polarizability which is important for the description of intermolecular interactions.

An attractive interaction was observed for all the tested orientations of the diacid whereas the size of the interaction energy was quite dependent on the relative orientation. For all orientations, the presence of an aerosol particle was found to cause a decrease of the mean static polarizability.

We found that the interaction energies are indistinguishable for dielectric constants in the interval  $\epsilon = 40\text{--}78.54$ .

A disadvantage inherent in the dielectric approximation is that the model only describes the formation of physisorbed states and does not account for the formation of chemical bonds. This is important in the description of growth and evaporation of organic aerosols because polar molecules such as succinic acid are likely to form hydrogen bonds to surface molecules in the aerosol particle.

The aerosol model could be improved by placing a number of water molecules on the surface of the dielectric medium and including these in an extended molecule approach.<sup>51,52</sup> Treating a few water molecules at the same level of theory as that for the molecular system would enable the description of short-range interactions important for the description of hydrogen bonds.

In the calculation of time-dependent properties, the heterogeneous solvation model does not account for the nonequilibrium situation arising from excitation of an electron. A more correct behavior may be introduced by dividing the polarization vector into an optical part that is assumed to respond instantaneously to changes in the molecular charge distribution and an inertial part describing the processes that are slow to relax.

This model enables investigations of molecules physisorbed on an aerosol particle. Our next step will be to compare the results reported here with those obtained using a QM/MM method<sup>18–20,53</sup> and thereby include chemisorption. This approach includes polarization as well as electrostatic interactions and a van der Waals term.

An obvious future goal is to relate the output of our models directly to experiments. One of the most promising methods for studying liquid surfaces and interfaces<sup>54</sup> is the experimental method vibrational sum frequency spectroscopy (VSFS). It has been used for probing the molecular structure and conformation of molecules at aqueous vapor–liquid interfaces. The technique is based on a second-order nonlinear optical process that directly probes the vibrational spectrum of molecules at an interface. The process is an allowed dipole transition in media that do not contain an inversion center, which is the case of molecules at an interface.<sup>54</sup> In our future work we will address VSFS of molecules at interfaces.

Finally, we will use a molecular reaction dynamics model to introduce kinetic energy terms for the nuclei and energy transfer between the aerosol particle and the molecule. This approach will lead to a theoretical procedure for the calculation of sticking coefficients. The dynamics of the nuclear motion will be described by classical mechanics, and the necessary potential energy surface will be calculated by the methods presented here along with the ones presented in ref 53. From the trajectory calculations, we will be able to calculate sticking coefficients and how the temperature affects the nuclear dynamics.

**Acknowledgment.** M.B. would like to thank the Danish Natural Science Council for support (Grant # 9901450). K.V.M. thanks the Danish Natural Science Research Council, the Danish Technical Research Council, the Danish Center for Scientific Computing, and the EU-network MOLPROP for support.

## References and Notes

- (1) Seinfeld, J. H.; Pandis, S. N. *Atmospheric Chemistry and Physics. From Air Pollution to Climate Change*; John Wiley & Sons: New York, 1998.
- (2) Pandis, S. N.; Russel, L. M.; Seinfeld, J. H. *J. Geophys. Res.* **1994**, *99*, 16945.
- (3) Clement, C. F.; Kulmala, M.; Vesala, T. *J. Aerosol Sci.* **1996**, *27*, 869.
- (4) Kulmala, M.; Wagner, P. E. *J. Aerosol Sci.* **2001**, *32*, 833.
- (5) Van Dingenen, R.; Raes, F. *Aerosol Sci. Technol.* **1991**, *15*, 93.
- (6) Ianni, J. C.; Bandy, A. R. *THEOCHEM* **2000**, 497, 19.
- (7) Arstila, H.; Laaksonen, K.; Laaksonen, A. *J. Chem. Phys.* **1998**, *108*, 1031.
- (8) Bandy, A. R.; Ianni, J. C. *J. Phys. Chem. A* **1998**, *102*, 6533.
- (9) Jayne, J. T.; Duan, S. X.; Davidovits, P.; Worsnop, D. R.; Zahniser, M. S.; Kolb, C. E. *J. Phys. Chem.* **1991**, *95*, 6329.
- (10) Davidovits, P.; Jayne, J. T.; Duan, S. X.; Worsnop, D. R.; Zahniser, M. S.; Kolb, C. E. *J. Phys. Chem.* **1991**, *95*, 6337.
- (11) Jørgensen, S.; Ratner, M. A.; Mikkelsen, K. V. *J. Chem. Phys.* **2001**, *115*, 3792.
- (12) Jørgensen, S.; Ratner, M. A.; Mikkelsen, K. V. *J. Chem. Phys.* **2001**, *115*, 8185.
- (13) Jørgensen, S.; Ratner, M. A.; Mikkelsen, K. V. *J. Chem. Phys.* **2002**, *116*, 10902.
- (14) Jørgensen, S.; Ratner, M. A.; Mikkelsen, K. V. *J. Chem. Phys.* **2002**, *116*, 53.
- (15) Kawamura, K.; Kaplan, I. R. *Environ. Sci. Technol.* **1987**, *21*, 105.
- (16) Satsumabayashi, H.; Kurita, H.; Yokouchi, Y.; Ueda, H. *Atmos. Environ.* **1990**, *24A*, 1443.
- (17) Sempere, R.; Kawamura, K. *Atmos. Environ.* **1994**, *28*, 449.
- (18) Warshel, A.; Levitt, M. *J. Mol. Biol.* **1976**, *103*, 227.
- (19) Poulsen, T. D.; Kongsted, J.; Osted, A.; Mikkelsen, K. V. *J. Chem. Phys.* **2001**, *115*, 2393.
- (20) Poulsen, T. D.; Ogilby, P.; Mikkelsen, K. V. *J. Chem. Phys.* **2002**, *116*, 3730.
- (21) Cui, Q.; Karplus, M. *J. Chem. Phys.* **2000**, *112*, 1133.
- (22) Cui, Q.; Karplus, M. *J. Phys. Chem. B* **2000**, *104*, 3721.
- (23) Miertus, S.; Scrocco, E.; Tomasi, J. *J. Chem. Phys.* **1981**, *55*, 117.
- (24) Miertus, S.; Tomasi, J. *J. Chem. Phys.* **1982**, *65*, 239.
- (25) Kirkwood, J. G. *J. Chem. Phys.* **1934**, *2*, 351.
- (26) Mikkelsen, K. V.; Ågren, H.; Jensen, H. J. A.; Helgaker, T. *J. Chem. Phys.* **1988**, *89*, 3086.
- (27) Rinaldi, D.; Ruiz-Lopez, M. F.; Rivail, J.-L. *J. Chem. Phys.* **1983**, *78*, 834.
- (28) Mikkelsen, K. V.; Dalgaard, E.; Svanstrøm, P. *J. Phys. Chem.* **1987**, *91*, 3081.
- (29) Ågren, H.; Medina-LLanos, C.; Mikkelsen, K. V. *J. Chem. Phys.* **1987**, *115*, 43.
- (30) Christiansen, O.; Mikkelsen, K. V. *J. Chem. Phys.* **1999**, *110*, 8348.
- (31) Mikkelsen, K. V.; Jørgensen, P.; Jensen, H. J. A. *J. Chem. Phys.* **1994**, *100*, 6597.
- (32) Cioslowski, J. *J. Phys. Rev. Lett.* **1989**, *62*, 1469.
- (33) Cioslowski, J. *J. Am. Chem. Soc.* **1989**, *111*, 8333.
- (34) Olsen, J.; Jørgensen, P. *J. Chem. Phys.* **1985**, *82*, 3235.
- (35) Jørgensen, P.; Jensen, H. J. A.; Olsen, J. *J. Chem. Phys.* **1988**, *89*, 3654.
- (36) Olsen, J.; Jensen, H. J. A.; Jørgensen, P. *J. Comput. Phys.* **1988**, *74*, 265.
- (37) Hetta, H.; Jensen, H. J. A.; Olsen, J.; Jørgensen, P. *J. Chem. Phys.* **1992**, *97*, 1174.
- (38) Bishop, D. M. *Adv. Quantum Chem.* **1994**, *25*, 1.
- (39) Shelton, D. P.; Rice, J. E. *Chem. Rev.* **1994**, *94*, 3–29.
- (40) Kanis, D.; Ratner, M. A.; Marks, T. J. *Chem. Rev.* **1994**, *94*, 195–242.
- (41) Hammond, B. L.; Rice, J. E. *J. Chem. Phys.* **1992**, *97*, 1138.
- (42) Karna, S. P.; Talapatra, G. B.; Wijekoon, W. M. K. P.; Prasad, P. N. *J. Phys. Rev. A* **1992**, *45*, 2763.
- (43) Sekino, H.; Bartlett, R. J. *J. Chem. Phys.* **1993**, *98*, 3022.
- (44) Jonsson, D.; Norman, P.; Ågren, H. *J. Chem. Phys.* **1996**, *105*, 581.
- (45) Jonsson, D.; Norman, P.; Ågren, H. *J. Chem. Phys.* **1996**, *105*, 6401.
- (46) Olsen, J.; Jørgensen, P. *J. Chem. Phys.* **1985**, *82*, 3235.
- (47) Chattaraj, P. K.; Sengupta, S. *J. Phys. Chem.* **1996**, *100*, 16126.
- (48) Helgaker, T.; Jensen, H. J. A.; Jørgensen, P.; Olsen, J.; Ruud, K.; Ågren, H.; Auer, A. A.; Bak, K. L.; Bakken, V.; Christiansen, O.; Coriani, S.; Dahle, P.; Dalskov, E. K.; Enevoldsen, T.; Fernandez, B.; Hättig, C.; Hald, K.; Halkier, A.; Heiberg, H.; Hetta, H.; Jonsson, D.; Kirpekar, S.; Kobayashi, R.; Koch, H.; Mikkelsen, K. V.; Norman, P.; Packer, M. J.; Pedersen, T. B.; Ruden, T. A.; Sanchez, A.; Saue, T.; Sauer, S. P. A.; Schimmelpfennig, B.; Sylvester-Hvid, K. O.; Taylor, P. R.; Vahtras, O. *Dalton, an ab initio electronic structure program*, Release 1.2; 2001; see <http://www.kjemi.uio.no/software/dalton/dalton.html>.
- (49) Christiansen, O.; Mikkelsen, K. V. *J. Chem. Phys.* **1999**, *110*, 1365.
- (50) Nielsen, C. B.; Sauer, S. P. A.; Mikkelsen, K. V. *J. Chem. Phys.* **2001**, *114*, 7753.
- (51) Yaliraki, S. N.; Roitberg, A. E.; Gonzalez, C.; Mujica, V.; Ratner, M. A. *J. Chem. Phys.* **1999**, *111*, 6997.
- (52) Xue, Y.; Datta, S.; Hong, S.; Reifenberger, R.; Henderson, J. I.; Kubiak, C. P. *J. Phys. Rev. B* **1999**, *59*, R7852.
- (53) Sloth, M.; Bilde, M.; Mikkelsen, K. V. *J. Chem. Phys.* **2003**, *118*, 22.
- (54) Richmond, G. L. *Annu. Rev. Phys. Chem.* **2001**, *52*, 357.